JACS
JOURNAL OF THE AMERICAN CHEMICAL SOCIETY
Article
pubs.acs.org/JACS

Excited-State Dynamics Achieved Ultimate Stereocontrol of Photocyclodimerization of Anthracenecarboxylates on a Glucose Scaffold

Gaku Fukuhara,* Kazuhiro Iida, Yuko Kawanami, Hidekazu Tanaka, Tadashi Mori, and Yoshihisa Inoue*

Department of Applied Chemistry, Osaka University, 2-1 Yamada-oka, Suita 565-0871, Japan

Supporting Information

ABSTRACT: Near-perfect stereoselectivity was attained in the diastereodifferentiating [4 + 4] photocyclodimerization of 2-anthracenecarboxylates tethered to a glucose scaffold not by thermodynamically tuning the conformer equilibrium in the ground state but by kinetically controlling the conformer dynamics and reactivity in the excited state, which enabled us, after removal of the scaffold, to obtain a single enantiomer of chiral *anti-head-to-head*-cyclodimer in >99% optical and 96% chemical yield from an ensemble of four precursor conformers.

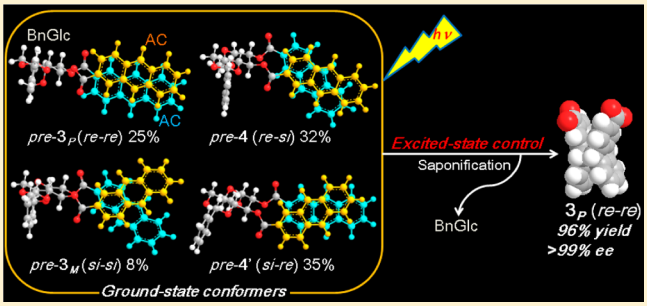

INTRODUCTION

Simultaneously achieving high chemical and optical yields in chiral photoreactions has long been an important goal for photo- and synthetic chemists.[1] Indeed, a number of diastereodifferentiating photoreactions, using diverse chiral auxiliaries and scaffolds, were examined[1] and several of them have been employed in the syntheses of crucial chiral components of bioactive natural products.[1f,2] Nevertheless, the high diastereomeric excesses (de's) reported are often accompanied by modest chemical yields, which is in contrast to the success in thermal asymmetric syntheses using chiral catalysts and enzymes.[3] For instance, moderate−high diastereoselectivities were reported for the photocyclization of diarylethenes (28−100% de),[4] the photoisomerization of cyclooctene (21−43% de),[5] the photocyclodimerization of cinnamates (46−97% de),[6] the photocycloaddition of enones to olefins (56−91% de),[7] and the Paternò−Büchi reaction of ketones with olefins (7−97%),[8] but high chemical yields have rarely been achieved simultaneously. This apparent trade-off does not appear to be inherent to photochirogenesis but is rather ascribed to an incomplete understanding of the mechanism and intermediates involved in the chirogenic processes occurring in the excited state,[6b,c,7g,8j] and also to the lack of practical methodology for controlling the stereochemical fate of the excited-state species.

This ultimate goal has however been reached recently through the supramolecular approach using cyclodextrin,[9] chiral Lewis acid,[10] chiral hydrogen-bonding template,[11] and serum albumin.[12] The main strategy employed in these studies is to confine the photosubstrate in the chiral environment of supra- or biomolecular host to reduce the conformational flexibility in such a way that the substrate exclusively exposes one of its prochiral enantio- or diastereotopic faces. In this strategy, the stereochemical fate of photochirogenic reaction relies primarily on the ground-state thermodynamics and therefore a sophisticated host design is required to optimize the stereochemical outcome.

We have investigated the diastereodifferentiating [4 + 4] photocyclodimerization of 2-anthracenecarboxylate (AC) tethered to linear polysaccharide and cyclic oligosaccharide scaffolds such as dimethylcellulose,[13a] amylose,[13b] α-cyclodextrin,[9] and cyclic nigerosylnigerose (CNN)[13c,d] (Scheme 1) to obtain (after saponification) *anti-head-to-head*-cyclodimer (*anti*-HH) **3** of 5−22% enantiomeric excess (ee) for dimethylcellulose, 1−10% ee for amylose, 8−90% for cyclo-

Scheme 1. Diastereodifferentiating Photocyclodimerization of 2-Anthracenecarboxylate (AC) Tethered to Chiral Scaffold (R*)

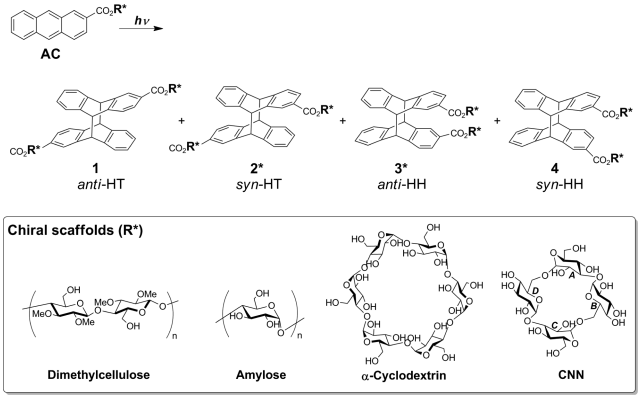

Received: September 17, 2015
Published: November 13, 2015

DOI: 10.1021/jacs.5b09775
J. Am. Chem. Soc. 2015, 137, 15007−15014

dextrin, and 99% ee for CNN in good-high chemical yields. In particular, the use of CNN scaffold, to which two ACs were introduced at the vicinal 2,3-diol of glucose ring B (**AC$_2$-CNN**; Figure 1), enabled us to obtain essentially enantiopure **3** (>99% ee) in 96% yield. Two major factors were thought crucial in achieving the ultimate stereoselectivity: (1) two ACs tethered in HH fashion to a vicinal 2,3-diol of CNN and (2) the CNN skeleton conformationally fixed by the water-bridged transannular hydrogen-bonding network on the back side.[14] The only detractive feature of this photochirogenesis is the difficulty encountered in preparing the starting material (**AC$_2$-CNN**), which was isolated in 1% yield from a complex mixture of mono- and di-AC esters of CNN.[13d]

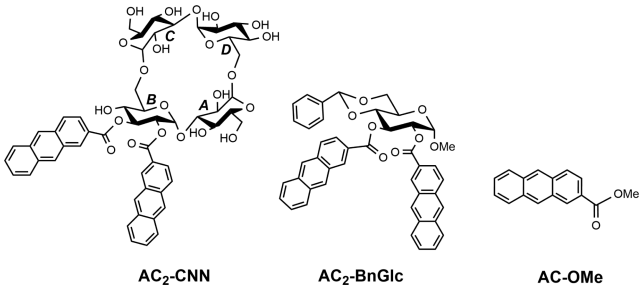

Figure 1. Structures of **AC$_2$-CNN**, **AC$_2$-BnGlc**, and **AC-OMe**.

In this study, we scrutinized whether this well-established, rather static, strategy is the only available and most efficient tool for optimizing the photochirogenic outcomes or any other dynamic mechanism operative in the excited state can more straightforwardly achieve the ultimate stereoselectivity in photochirogenesis. Close photophysical and photochemical studies on the diastereodifferentiating photocyclodimerization of 2-anthracenecarboxylates tethered to a simple glucose scaffold revealed that a more dynamic approach enables us to reach the ultimate goal of photochirogenesis, affording a single enantiomer of *anti*-HH cyclodimer in 96% yield after removal of the scaffold without using a designer scaffold.

RESULTS AND DISCUSSION

Synthesis and Chiroptical Properties of Methyl 2,3-Di-*O*-(2-anthroyl)-4,6-*O*-benzylidene-α-D-glucopyranoside (AC$_2$-BnGlc). Esterification of methyl 4,6-*O*-benzylidene-α-D-glucopyranoside (BnGlc)[15] with 2-anthracenecarboxylic acid (2.2 equiv) was performed in dry DMF with 1-ethyl-3-(3′-dimethylaminopropyl)carbodiimide hydrochloride (EDC) and *N*,*N*-dimethylamino-4-pyridine (DMAP) to afford the desired photosubstrate, methyl 2,3-di-*O*-(2-anthroyl)-4,6-*O*-benzylidene-α-D-glucopyranoside (**AC$_2$-BnGlc**; Figure 1), in 63% isolated yield (see the Supporting Information (SI)), which is much better than the 1% yield reported for **AC$_2$-CNN**[13c,d] and is acceptable as a starting material of the photochirogenic reaction.

The chiroptical properties of **AC$_2$-BnGlc** were examined by UV−vis and circular dichroism (CD) spectroscopies, and the results were compared with those of **AC$_2$-CNN** reported earlier[13c,d] and methyl 2-anthracenecarboxylate (**AC-OMe**) as a reference. As can be seen from Figure 2 (top), when compared with reference **AC-OMe**, the main ^1B_b transition at ca. 250 nm is significantly band-broadened and the lowest-energy ^1L_b transition[16] is bathochromically shifted by 4−6 nm in **AC$_2$-BnGlc** and **AC$_2$-CNN**, suggesting π−π interactions between the two AC chromophores introduced at the vicinal 2,3-positions of glucose. Also, in the ^{1}H NMR spectrum, all of the aromatic protons of **AC$_2$-BnGlc** were modestly upfield-shifted by 0.05−0.17 ppm (Table S1 in SI) in comparison with the corresponding protons of **AC-OMe**, implying weak π−π interactions in **AC$_2$-BnGlc**. The circular dichroism (CD) spectrum (Figure 2, middle) as well as the anisotropy ($g = \Delta\varepsilon/\varepsilon$) spectrum (Figure 2, bottom) of **AC$_2$-BnGlc** are practically superimposable on those of **AC$_2$-CNN**, despite the somewhat different solvents used (CH_3CN versus CH_3CN−H_2O). According to the exciton chirality theory,[17] the positive exciton couplet observed indicates a right-handed helical arrangement of the two AC chromophores in both **AC$_2$-BnGlc** and **AC$_2$-CNN**, which is in agreement with the $2_{eq}3_{eq}$-conformation adopted by the D-glucose scaffold.

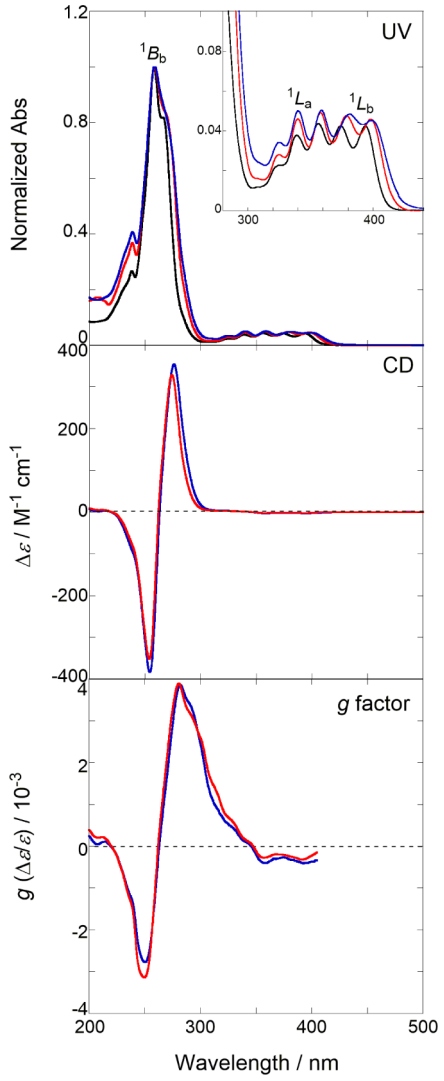

Figure 2. UV−vis (top) spectrum of **AC-OMe** (20 μM) in CH_3CN (black), and UV−vis (top), CD (middle), and anisotropy ($g = \Delta\varepsilon/\varepsilon$) spectra (bottom) of **AC$_2$-BnGlc** (10 μM) in CH_3CN (red) and of **AC$_2$-CNN** (45 μM) in 45:55 CH_3CN−H_2O (blue), measured at 25 °C in a 1 cm cell.

Photophysical Behavior of AC$_2$-BnGlc. In this system, two AC chromophores are anchored to the $2_{eq}3_{eq}$-positions of BnGlc scaffold and hence more or less overlap with each other. The only difference among these conformers is the choice of the enantiotopic *re*/*si* faces confronting each other (the possible

DOI: 10.1021/jacs.5b09775
J. Am. Chem. Soc. 2015, 137, 15007−15014

conformers and their theoretical analyses will be presented below in Figure 6), which however makes the analysis of the excited-state behavior of each conformer significantly different from the standard model that deals with bichromophoric systems linked by a flexible oligomethylene chain.[18]

To elucidate the excited-state behavior, we measured the fluorescence spectrum and fluorescence lifetime of **AC_2-BnGlc** and compared the obtained results with those for **AC_2-CNN**[13c,d] and **AC-OMe**. As shown in Figure 3a (where the

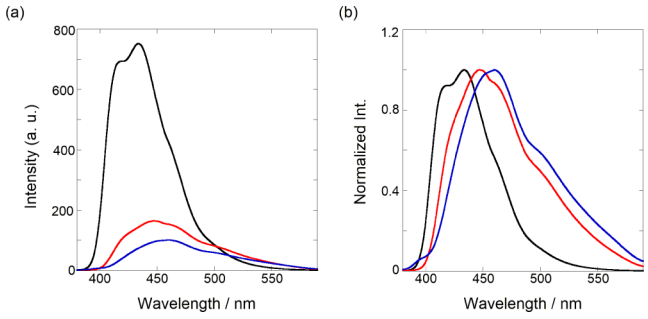

Figure 3. (a) Original and (b) normalized fluorescence spectra of **AC-OMe** (87 μM) in CH_3CN (black), **AC_2-BnGlc** (29 μM) in CH_3CN (red), and **AC_2-CNN** (25 μM) in 45:55 CH_3CN-H_2O (blue) at room temperature; the excitation wavelength was set at 300 nm, where these three solutions showed the identical absorbances.

same absorbance at the excitation wavelength was secured among the three solutions by tuning the concentration and excitation wavelength to allow direct comparison), the fluorescence intensity relative to that for **AC-OMe** was greatly reduced to 19% for **AC_2-BnGlc** and to 10% for **AC_2-CNN**. By comparing with the fluorescence quantum yield (Φ_f) of 0.62 reported for **AC-OMe**,[19] we approximated the Φ_f values as 0.12 for **AC_2-BnGlc** and as 0.062 for **AC_2-CNN** from the intensity ratios. These are appreciably smaller than the Φ_f value of 0.16 reported for 1,5-bis(2-anthroyloxy)pentane (**AC-O$(CH_2)_5$O-AC**), in which two AC chromophores are linked together with a longer flexible pentamethylene chain.[20] The smaller Φ_f values for **AC_2-BnGlc** and **AC_2-CNN**, compared with those for **AC-OMe** and **AC-O$(CH_2)_5$O-AC**, are attributable to the fast intramolecular photocyclodimerization of ACs on the scaffold. Indeed, the photocyclodimerization of **AC_2-BnGlc** turned out to proceed 90-fold faster than the intermolecular photocyclodimerization of **AC-OMe** at 10 μM (see Figure S7 in SI).

The normalized fluorescence spectra in acetonitrile (Figure 3b) revealed the less-structured, non-mirror-imaged features of the bichromophoric **AC_2-BnGlc** and **AC_2-CNN** fluorescence as well as the bathochromic shifts of the apparent peak maxima by 13 nm for **AC_2-BnGlc** and 26 nm for **AC_2-CNN** with accompanying additional emission at longer wavelengths (450–600 nm). These bathochromic shifts are much larger than the 4–6 nm shifts found in the UV–vis spectra (Figure 2), indicating considerable conformational relaxation from the Franck–Condon state on the excited-state potential surface. The red-shifted and band-broadened fluorescence is assigned not to an excited state of the π-stacked AC dimer complex formed in the ground state, but rather to a conformer ensemble of intramolecular AC excimers formed upon relaxation from the Franck–Condon state. This is because the excitation spectra monitored at various wavelengths across the fluorescence spectral region of **AC_2-BnGlc** exactly matched to each other and were superimposable on the UV–vis spectrum; see Figure S8 in SI. If any emission arose from the excited state of a π-stacked ground-state complex, the excitation spectra monitored at longer wavelengths should exhibit appreciable deviations from the UV–vis and other excitation spectra, since such a π-stacked complex should absorb at appreciably longer wavelengths than less- or nonstacked ground-state conformers.

More intriguingly, the bathochromic shifts observed for **AC_2-CNN** (26 nm) and in particular for **AC_2-BnGlc** (13 nm) are much smaller than the 100 nm shift reported for a typical sandwich excimer of unsubstituted anthracene.[21] This smaller shift or "insufficient" relaxation for the excimer emission is likely to arise from the conformational restriction encountered upon relaxation on the BnGlc scaffold, and therefore each of the ground-state conformers (which are illustrated in Figure 6) undergoes more or less insufficient relaxation to the corresponding excimer, which may be called a "suspended" or "frustrated" excimer. Some of them may be less-stacked and fluoresce without giving the cyclodimers, but if the geometry allows more stacked, less frustrated, excimer(s) may spontaneously cyclodimerize without emitting light.

In such a situation, highly reactive excimer(s) (such as *pre*-3_P* shown in Figure 6) may function as photochemical drain(s) in the excited-state landscape and the apparent fluorescence behavior becomes simpler than anticipated, involving essentially two fluorescent species (i.e., *pre*-3_M* and nearly degenerated *pre*-**4***/*pre*-**4′*** shown in Figure 6 and Scheme 2).

Scheme 2. Plausible Mechanism of Diastereodifferentiating Photocyclodimerization of 2-Anthracenecarboxylates on the BnGlc Scaffold

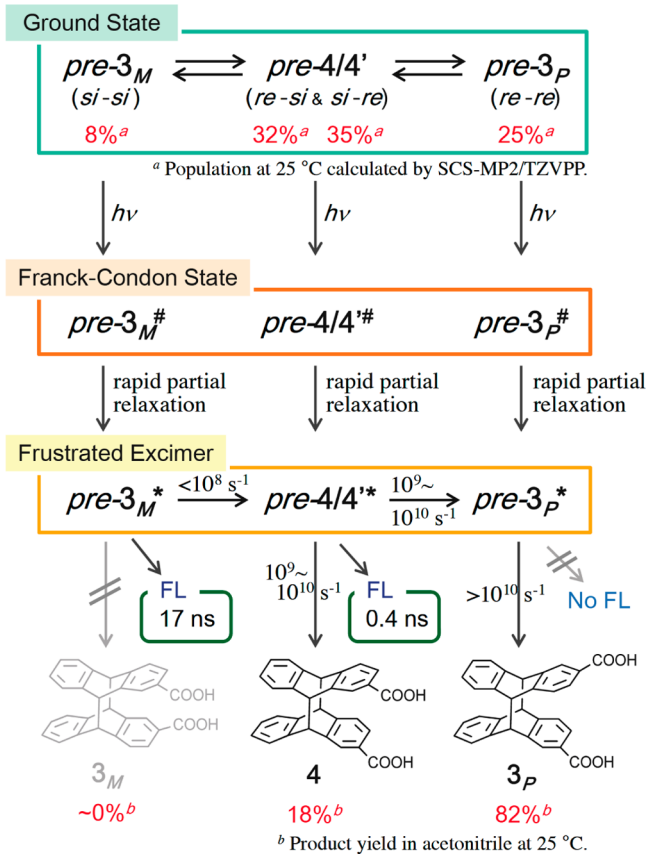

DOI: 10.1021/jacs.5b09775
J. Am. Chem. Soc. 2015, 137, 15007–15014

Table 1. Fluorescence Lifetimes of AC-OMe, AC_2-BnGlc, and AC_2-CNN[a]

compd.	solvent	λ_{em}[b]	n[c]	τ_1	A_1	τ_2	A_2	τ_3	A_3	χ^2
AC-OMe	CH_3CN	450	1	13.6						1.2
		520	1	13.5						1.2
AC_2−BnGlc	CH_3CN	420	2	0.4	0.83	16.9	0.17			1.2
		450	2	0.4	0.72	17.3	0.28			1.1
		500	2	0.7	0.27	17.9	0.73			1.1
				0.4[d]	0.41	17.8	0.59			1.1
		520	2	0.8	0.17	17.8	0.83			1.2
				0.4[d]	0.23	17.7	0.77			1.2
AC_2−CNN[e]	[f]	450	3	0.4	0.85	4.9	0.11	19.5	0.04	1.0
		515	3	0.4	0.52	5.2	0.43	19.0	0.05	1.1

[a]Fluorescence lifetime (τ_i/ns) and relative abundance (A_i) of each component determined by the single photon counting method in nondegassed solution at room temperature; error ±0.1 ns. [b]Monitoring wavelength in nm. [c]Number of components. [d]The effect of fixing τ_1 at 0.4 ns (the τ_1 value obtained upon monitoring at 420 and 450 nm) was examined to find no essential differences in τ, A, or χ^2, and hence the results obtained by free fitting were employed; the deviations are considered to represent the experimental error particularly for short lifetimes <1 ns. [e]Cited from references13c, d. [f]CH_3CN−H_2O (45:55).

Table 2. Distribution of Cyclodimers 1−4 and Enantiomeric Excess of Cyclodimer 3 Obtained in the Photocyclodimerization of AC_2-BnGlc Followed by Saponification[a]

					product distribution/% (*ee*/%)[d]				
solvent	E_T[b]	concentration/μM	temperature/°C	conversion/%[c]	**1**	**2**	**3**	**4**	**3/4**
toluene	33.9	10	25	99	<0.1	0.1	75.0 (−99.9)	24.8	3.0
THF	37.4	10	50	98	0.1	0.1	78.6 (−99.9)	21.2	3.7
			25	93	0.1	0.1	79.2 (−99.9)	20.6	3.8
			0	95	0.1	0.1	80.4 (−99.9)	19.4	4.1
			−50	76	0.1	0.1	84.1 (−99.9)	15.7	5.4
CH_2Cl_2	41.1	10	25	92	0.1	<0.1	82.2 (−99.9)	17.7	4.6
CH_3CN	46.0	1	25	77	<0.1	<0.1	81.9 (−99.3)	17.9	4.6
		10	25	98	0.1	<0.1	81.6 (−99.9)	18.2	4.5
		100	25	98	0.7	0.6	80.8 (−99.9)	17.9	4.5
EtOH	51.9	10	25	92	0.2	0.1	85.2 (−99.9)	14.5	5.9
CH_3OH	55.5	1	50	71	0.1	<0.1	88.5 (−99.9)	11.4	7.8
			25	95	<0.1	<0.1	89.7 (−99.9)	10.2	8.8
			0	59	0.1	<0.1	91.2 (−99.9)	8.6	10.6
			−50	48	0.6	0.3	94.1 (−99.0)	5.0	18.8
			−70	31	0.1	0.1	96.0 (−99.8)	3.8	25.3
CH_3OH−H_2O (9:1)		10	25	89	0.1	0.1	92.8 (−99.8)	7.0	13.3

[a]Irradiated at 360 ± 10 nm under N_2 for 25 min with a 300-W xenon lamp through a band-pass filter. [b]Dimroth and Reichardt's solvent polarity parameter in kcal mol^{-1} (ref 23). [c]Conversion determined by monitoring the absorbance change after irradiation. [d]Irradiated sample was saponified (with aqueous KOH for 1 h) and then subjected to chiral HPLC (ODS + Chiralcel OJ-RH) for product distribution and ee; the negative sign for ee indicates dominant formation of the second-eluted (*P*)-enantiomer (ref 24). The ee of **2** was not determined because of the very small areas of its enantiomer peaks upon HPLC analysis, but appeared to be fairly low (<7.4%), as shown in Figure S11 in SI, suggesting its origin (the intermolecular photocyclodimerization; see text).

The fluorescence lifetime study revealed the existence of two fluorescing species of different lifetimes; i.e., a short-lived species emitting at shorter wavelengths and a long-lived species emitting at longer wavelengths. Thus, the fluorescence decay profiles of **AC_2-BnGlc** monitored at 420−520 nm were nicely fitted to a sum of two exponential functions (Figure S10 in SI), from which the lifetime (τ) and relative abundance (A) of each species were determined as shown in Table 1. The two lifetimes obtained, 0.4−0.8 ns and 16.9−17.9 ns, are distinctly different from that of **AC-OMe** (13.5−13.6 ns), suggesting that an excited AC in **AC_2-BnGlc** does not fluoresce but immediately interacts with the neighboring AC on the same scaffold to give an ensemble of intramolecular excimers in different conformations. Furthermore, the overlaid fluorescence decay profile of **AC_2-BnGlc** with that of **AC-OMe** (Figure S10g,h in SI) did not show any growth kinetics that can be ascribed to excimer formation. If one of the emissions arose from a monomer that rotates to form excimer, one would expect to see growth kinetics for the emission of the excimer. The shift in the emission spectra and the fact that the longer lifetime is more prominent at longer wavelengths (Table 1) are also consistent with the assignment of the emission from two excimers.

The rate of subsequent cyclodimerization should be critically influenced by the excimer conformation. Some of the conformers may spontaneously cyclodimerize without emitting light and hence are fluorometrically silent, while the rest of them may react slower and compete in rate with the emissive decay path, the ratio of which should depend on the inter-AC distance and angle in the relevant conformer.

From these considerations, we may assign the short- and long-lived species detected in the lifetime measurement to a more reactive, less emissive excimer and a more stable emissive excimer, respectively. As can be seen from Table 1, the relative abundance of the long-lived species (A_2) steadily increases from

DOI: 10.1021/jacs.5b09775
J. Am. Chem. Soc. 2015, 137, 15007−15014

17% to 83% at the expense of A_1 by shifting the monitoring wavelength from 420 to 520 nm, indicating that the long-lived excimer emits at longer wavelengths than the short-lived. It should be emphasized however that these emissive excimers are not the only species contributing to the photocyclodimerization but presumably a more important role is played by the nonemissive (fluorometrically silent), highly reactive conformer, which is experimentally supported by the fact that the fluorescence quantum yield of **AC$_2$-BnGlc** (Φ_f = 0.12) is substantially smaller than those reported for monochromophoric **AC-OMe** (Φ_f = 0.62)[19] and also for bichromophoric, but photochemically inert 1-anthroyloxy-2-benzoyloxy- and 1-anthroyloxy-2-naphthoyloxycyclohexanes (Φ_f = 0.50 and 0.65, respectively).[19] Furthermore, the number of emissive conformers is not necessarily restricted to two, since the fluorescent excimers of comparable lifetimes are not distinguishable in our measurements. Indeed, three emissive species of 0.4, 4.9−5.2, and 19.0−19.5 ns lifetimes have been observed for **AC$_2$-CNN** (Table 1).[13c,d]

Diastereodifferentiating Photocyclodimerization of AC$_2$-BnGlc. Photoirradiation of **AC$_2$-BnGlc** was performed at 360 nm in various solvents at temperatures ranging from +50 to −70 °C. The photolyzed sample was saponified with aqueous KOH to retrieve AC cyclodimers **1**−**4** as sole detectable products, which were subjected to chiral HPLC analysis to afford the results shown in Table 2.

The quantum yield of photocyclodimerization (Φ_c) was determined as 0.05 for **AC$_2$-BnGlc** in acetonitrile (Figure S9 in SI), which is appreciably smaller than the Φ_c value (0.107) reported for **AC-O(CH$_2$)$_5$O-AC** in dichloromethane,[20] probably due to the more rigid BnGlc linker/scaffold employed in the present system. It is also to note that the individual photocyclodimerization quantum yield of the *pre*-**3$_P$** conformer ($\Phi_c^{pre\text{-}3P}$) would be much larger (∼0.2) than that determined experimentally (Φ_c 0.05), since its population in the ground state is only 25% at 25 °C and 16% at −70 °C among the four conformers (Table S2 in SI) but this minor conformer explains most (80−96%) of the photocyclodimerization products.

Concentration Effects. In order to assess the possible contamination by the intermolecular photocyclodimerization of **AC$_2$-BnGlc**, which is expected to favor the formation of *head-to-tail* (HT) cyclodimers **1** and **2**,[22] we first examined the effect of substrate concentration on the product distribution. The photocyclodimerization of **AC$_2$-BnGlc** was performed at 1, 10, and 100 μM concentrations in acetonitrile at 25 °C to give the HT dimers in negligible yield (≤0.1%) at concentrations ≤10 μM (for the result at 10 μM, see Figure S11 in SI) but in slightly higher 0.6−0.7% yield at 100 μM. Nevertheless, the high chemical (81−82%) and optical (>99% ee) yields for **3**, as well as the high HH selectivity (≥99%), were not seriously deteriorated even at the highest concentration, demonstrating the excellent performance of the glucose skeleton as a chiral scaffold for the diastereodifferentiating photocyclodimerization of AC.

Solvent Effects. **AC$_2$-BnGlc** was soluble in a variety of solvents ranging from toluene to aqueous methanol, which allowed us to closely examine the effects of solvent and temperature on the product ratio and the ee of **3**. The results obtained provided us with mechanistically and synthetically crucial pieces of information described below.

As shown in Table 2, *anti*-HH **3** was consistently the dominant product (75−96% yield) and essentially enantiopure (>99% ee) in all the solvents examined. However, the *anti*/*syn*-HH, or **3**/**4**, ratio was sensitive to the solvent employed, being significantly enhanced from 3.0 (75% *anti*) in toluene and 3.8 (79% *anti*) in tetrahydrofuran (THF) to 8.8 (90% *anti*) in methanol and then to 13.3 (93% *anti*) in methanol−water (9:1) at 25 °C. This trend is difficult to rationalize by the solvation to substrate in the ground state, as the UV−vis and CD spectra were practically independent of the solvent polarity (Figure S12 in SI), implying nearly the same average conformation adopted in all the examined solvents, but is accounted for in terms of the solvation in the excited state. Indeed, the fluorescence spectrum of **AC$_2$-BnGlc** was highly solvent-dependent and gradually shifted to the longer wavelengths (with accompanying band-broadening) in the solvents of higher polarity (Figure S13 in SI), indicating substantial stabilization of the excimer ensemble in polar solvents, the degree of which may differ from conformer to conformer.

Intriguingly, the logarithm of **3**/**4** ratio was reasonably proportional to solvent polarity parameter E_T as shown in Figure 4. The overall Gibbs free energy difference for the formation of **3** versus **4** can be calculated from the temperature dependence of the **3**/**4** ratio by using the differential Gibbs−Helmholtz equation, $-\Delta\Delta G_{3-4} = RT \ln(\mathbf{3}/\mathbf{4})$ where T = 298 K, as 2.7 and 3.3 kJ mol^{-1} in less polar toluene and THF, respectively, but much larger 5.4 and 6.4 kJ mol^{-1} in polar methanol and aqueous methanol, respectively.

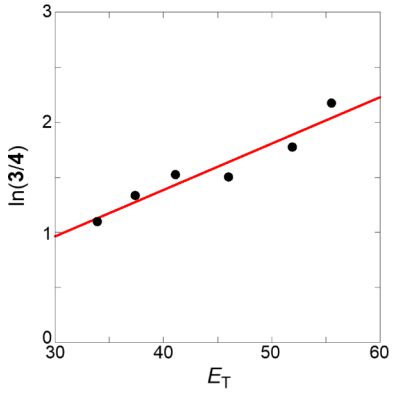

Figure 4. Plot of the logarithm of *anti*/*syn*, or **3**/**4**, ratio against the Reichardt's E_T value of solvent (from toluene to methanol); correlation coefficient; r 0.95.

Temperature Effects. The effects of temperature on the **3**/**4** ratio and the ee of **3** were examined in THF and methanol at temperatures ranging from +50 to −50 or −70 °C; the results are listed in Table 2. As was the case with the solvent effects, the ee of **3** was kept high (>99%) in both THF and methanol at all the temperatures examined, while the **3**/**4** ratio was a critical function of temperature, increasing with decreasing temperature to reach 5.4 in THF at −50 °C and 25.3 in methanol at −70 °C. Thus, **AC$_2$-BnGlc** enabled us to reach the ultimate goal by affording enantiopure **3** in 96% yield in methanol at −70 °C without using the difficultly prepared starting material **AC$_2$-CNN**.

Since the **3**/**4** ratio was consistently kept high at >7.8 in methanol even at ambient temperatures (Table 2), we performed the preparative-scale photocyclodimerization of **AC$_2$-BnGlc** in methanol at 50 °C (for better solubilities of the starting material as well as the photocyclodimerization products) to obtain essentially enantiopure **3$_P$** (97% chemical

DOI: 10.1021/jacs.5b09775
J. Am. Chem. Soc. 2015, 137, 15007−15014

purity and 99.6% ee) in 81% isolated yield after removal of the BnGlc scaffold by saponification (see SI).

The significant temperature dependence of the **3**/**4** ratio does not appear to originate from the conformational change of substrate in the ground state, as the anisotropy spectra obtained at different temperatures (which are dimensionless ($g = \Delta\varepsilon/\varepsilon$) and hence intrinsically corrected for the volume changes caused by temperature variation) were practically superimposable (Figure S17 in SI). Hence, the temperature-dependent **3**/**4** ratios were subjected to the Eyring analysis for a more quantitative evaluation of the enthalpic and entropic contributions to the anti/syn selectivity upon HH photocyclodimerization on the glucose scaffold. As shown in Figure 5, the logarithms of the **3**/**4** ratios obtained in THF and in methanol were plotted against the inverse temperature to afford good straight lines of distinctly different slopes and intercepts. From the slope and intercept, the differential activation enthalpy ($\Delta\Delta H^{\ddagger}_{3-4}$) and entropy ($T\Delta\Delta S^{\ddagger}_{3-4}$, T = 298 K) for the anti/syn selective process were calculated as −2.4 kJ mol^{-1} and 1.0 kJ mol^{-1} for THF and as −5.4 kJ mol^{-1} and 0.0 kJ mol^{-1} for methanol. These results reveal that the high *anti*-HH selectivity achieved is exclusively enthalpy-driven in methanol but attributable to the major enthalpic and minor entropic gains in THF. The nil or minor contribution of entropy may indicate the limited roles of conformational freedom and solvation played in the anti/syn selective process.

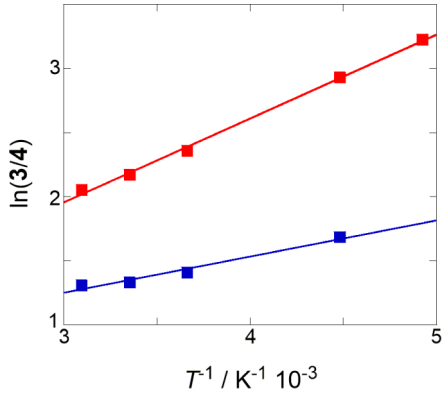

Figure 5. Eyring plots of the **3**/**4** ratios obtained in THF (blue) and in methanol (red); r 0.99 in both cases.

Origin of the Stereoselectivity. In this diastereodifferentiating photocyclodimerization, the *re*- and *si*-faces of prochiral 2-anthracenecarboxylate (AC) moiety are differentiated by the chiral glucose scaffold upon photocyclodimerization to **3** and **4**. Two AC moieties approaching from their *re*-faces (*re-re* approach) give (*P*)-enantiomer of **3** (**3**$_P$) and the *si-si* attack leads to antipodal (*M*)-enantiomer of **3** (**3**$_M$), while the *re-si* and *si-re* approaches lead to achiral **4**.[24] Hence, knowing the absolute configuration of dominant product **3** is indispensable for discussing the origin of the excellent diastereoselectivity attained. In a previous study,[24] we have determined the absolute configurations of the enantiomers of **3** first- and second-eluted from a tandem HPLC column of ODS and chiral OJ-RH by comparing the experimental CD spectra of both fractions with the theoretical ones. By exploiting this correlation between the absolute configuration and the elution order on the same chiral column, the dominant enantiomer obtained in the present study was unequivocally assigned to **3**$_P$. This means that the *re-re* approach is thermodynamically and/or kinetically highly favored over the *si-si* and *re-si*/*si-re* approaches upon photocyclodimerization.

In principle, the product distribution and diastereoselectivity are controlled potentially by the ground-state equilibrium among the *re-re*, *si-si*, *re-si*, and *si-re* conformers (which are precursors to **3**$_P$, **3**$_M$, **4**, and again **4** and hence termed *pre*-**3**$_P$, *pre*-**3**$_M$, *pre*-**4**, and *pre*-**4**′, respectively) and also by the excited-state equilibrium, lifetime, and reactivity of these conformers. Accordingly, we first evaluated the conformer distribution of **AC$_2$-BnGlc** in the ground state theoretically by density functional theory (DFT) calculations and experimentally by CD spectroscopy. The preliminary conformer search was performed by using MM2 in Chem3D and the most stable eight conformers obtained were subjected to the geometry optimization and energy calculation by the DFT method at the D3-B-LYP/TZVP level and also at higher SCS-MP2/TZVPP level (Table S2 in SI).[25] By using the result of more accurate latter calculation, the Boltzmann population of *pre*-**3**$_M$, *pre*-**3**$_P$, *pre*-**4**, and *pre*-**4**′ was calculated as 8:25:32:35 at 25 °C (Figure 6). If the product ratio is determined solely by the ground-state thermodynamics, this population predicts a **3**/**4** ratio of 0.49 and −52% ee for **3**, which however disagree with the experimental values, i.e., **3**/**4** = 3.0−13.3 and −99% ee, indicating that the subsequent excited-state processes are responsible for the high stereoselectivities. Furthermore, the electronic transition moments of the two AC moieties on the scaffold (indicated by arrows in Figure 6) are twisted clockwise (with twist angles of 18−42°) in all the conformers, predicting an intense positive exciton couplet in CD spectrum, which is in nice agreement with the huge positive couplet of up to 680 M^{-1} cm^{-1} amplitude observed in various solvents (Figure 2).

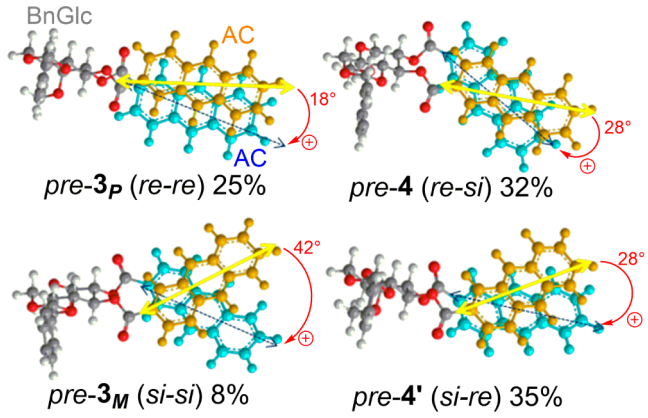

Figure 6. *Pre*-**3**$_P$ (*re-re*), *pre*-**3**$_M$ (*si-si*), *pre*-**4** (*re-si*), and *pre*-**4**′ (*si-re*) conformers of **AC$_2$-BnGlc** geometry-optimized by the DFT-D3-B-LYP/TZVP calculation and the Boltzmann population at 25 °C on the basis of their relative energies calculated by DFT-SCS-MP2/TZVPP.

The conformer ratio in the ground state should be preserved upon Franck−Condon excitation and immediately after the subsequent spontaneous relaxation to the corresponding excited-state conformer ensemble of *pre*-**3**$_M$*, *pre*-**3**$_P$*, *pre*-**4***, and *pre*-**4**′*. This conformer ensemble repopulates (as far as the lifetime allows) in the excited state in competition with other physical and chemical decay processes, including fluorescence and cyclodimerization, as illustrated in Scheme 2.

In determining the photophysical and photochemical fates of each excited-state conformer, the ground-state conformation is considered to play some roles. Thus, the dominant formation of

DOI: 10.1021/jacs.5b09775
J. Am. Chem. Soc. 2015, 137, 15007−15014

3_P is rationalized at least in part by the ground-state conformation of its precursor *pre*-3_P, which if photochemically inert would lead to the longest-lived excimer upon excitation but is in reality highly photocyclodimerizable, possessing the largest π-overlap and the shortest distances between the 9,10-positions of two facing AC moieties. On the contrary, *pre*-3_M* and *pre*-**4**/**4**′*, carrying more twisted AC moieties, are not suitable for geometrical reasons for immediate cyclodimerization without significantly changing the original conformation and hence have better chances to fluoresce or isomerize to *pre*-**4**/**4**′* and *pre*-3_P*, the latter of which instantaneously cyclodimerizes to afford 3_P without emitting light (at least at a rate beyond the detection limit of our instrument (~0.1 ns) or $>10^{10}$ s^{-1}), while the former can cyclodimerize, fluoresce, or isomerize to the latter at comparable rates in the order of 10^9−10^{10} s^{-1} estimated from the fluorescence lifetime (0.4−0.8 ns). On the other hand, *pre*-3_M* cannot cyclodimerize due to the strain induced upon cyclodimerization and hence fluoresces (τ 16.9−17.9 ns) or may isomerize to *pre*-**4**/**4**′* at a much slower rate ($<10^8$ s^{-1}) than that for the isomerization of *pre*-**4**/**4**′* to *pre*-3_P* (10^9−10^{10} s^{-1}). The backward transformations from fast reacting *pre*-3_P* to moderately reacting *pre*-**4**/**4**′* and then to unreactive *pre*-3_M* are negligible or very slow (meaning that no full equilibria are established within the excited-state lifetime) to allow *pre*-3_M* and *pre*-**4**/**4**′* to independently fluoresce. This scenario can rationalize the dominant formation of 3_P in 75−93% in various solvents from toluene to aqueous methanol at 25 °C, which far exceed the ground-state population of *pre*-3_P (25%), as well as the only two fluorescent species of 0.4−0.8 ns and 16.9−17.9 ns lifetimes detected experimentally (Table 1) and their assignment to *pre*-**4**/**4**′* and *pre*-3_M*, respectively. This is because the former conformers, both carrying two modestly twisted AC moieties, can cyclodimerize at slower rates than *pre*-3_P* and hence is likely to emit short-lived fluorescence, while the latter hardly cyclodimerizes due to the conformational restriction of the glucose scaffold and emits long-lived fluorescence. Furthermore, the favored formation of **3** and the higher ee in polar/protic solvents are reasonably accounted for in terms of the solvo/hydrophobic effect on the excimer ensemble, which drives the isomerization to the most stacked *pre*-3_P* to maximize the **3**/**4** ratio as well as the ee in aqueous methanol at 25 °C and in methanol at −70 °C.

CONCLUSION

In this study, we employed simple glucose scaffold BnGlc for the diastereodifferentiating photocyclodimerization of AC as a synthetically convenient yet photochirogenically efficient alternative to more sophisticated cyclic oligosaccharides such as cyclodextrin and CNN and obtained a single enantiomer 3_P (>99% ee) after removal of the scaffold, irrespective of the solvent and temperature used, in high chemical yields of 96% at −70 °C (in methanol) and 93% even at 25 °C (in aqueous methanol). The combined theoretical and photophysical studies revealed that the second minor conformer *pre*-3_P is conformationally most photocylodimerizable, while the other *pre*-3_M and *pre*-**4**/**4**′ conformers are totally photoinert or less photoreactive and hence converge to *pre*-3_P* in the excited state to afford 3_P predominantly. We may conclude therefore that the dynamic excited-state isomerization and the subsequent cyclodimerization kinetics can overwhelm the thermodynamically determined conformer population in the ground state. The present study not only elucidate the factors and mechanisms operative in the diastereodifferentiating photocyclodimerization but also provides us with a new concept and versatile tools to overcome the unfavorable ground-state thermodynamics and dynamically control the stereochemical outcomes of photochirogenic reactions.

ASSOCIATED CONTENT

Supporting Information

The Supporting Information is available free of charge on the ACS Publications website at DOI: 10.1021/jacs.5b09775.

Detailed experimental procedures, synthesis and characterization of **AC_2-BnGlc**, quantum yield determination, preparative-scale irradiation, and theoretical calculations. (PDF)

AUTHOR INFORMATION

Corresponding Authors

*gaku@chem.eng.osaka-u.ac.jp

*inoue@chem.eng.osaka-u.ac.jp

Notes

The authors declare no competing financial interest.

ACKNOWLEDGMENTS

This work was supported by Grant-in-Aid for Young Scientists (B) (No. 23750129) to G.F. and Grant-in-Aid for Scientific Research (A) (No. 21245011) to Y.I. both from JSPS, and a grant from The Sumitomo Foundation to G.F., all of which are gratefully appreciated.

REFERENCES

(1) (a) Rau, H. *Chem. Rev.* **1983**, *83*, 535. (b) Inoue, Y. *Chem. Rev.* **1992**, *92*, 741. (c) Griesbeck, A. G.; Meierhenrich, U. J. *Angew. Chem., Int. Ed.* **2002**, *41*, 3147. (d) Inoue, Y.; Ramamurthy, V. *Chiral Photochemistry*; Marcel Dekker: New York, 2004. (e) Müller, C.; Bach, T. *Aust. J. Chem.* **2008**, *61*, 557. (f) Hoffmann, N. *Chem. Rev.* **2008**, *108*, 1052. (g) Ramamurthy, V.; Inoue, Y. *Supramolecular Photochemistry*; Wiley: Hoboken, NJ, 2011. (h) Yang, C.; Inoue, Y. *Chem. Soc. Rev.* **2014**, *43*, 4123. (i) Yan, Z.; Wu, W.; Yang, C.; Inoue, Y. *Supramol. Catal.* **2015**, *2*, 9.

(2) (a) Crimmins, M. T. *Chem. Rev.* **1988**, *88*, 1453. (b) Winkler, J. D.; Bowen, C. M.; Liotta, F. *Chem. Rev.* **1995**, *95*, 2003.

(3) (a) Knowles, W. S. *Angew. Chem., Int. Ed.* **2002**, *41*, 1998. (b) Noyori, R. *Angew. Chem., Int. Ed.* **2002**, *41*, 2008. (c) Sharpless, K. B. *Angew. Chem., Int. Ed.* **2002**, *41*, 2024. (d) *Asymmetric Organic Synthesis with Enzymes*; Gotor, V., Alfonso, A., García-Urdiales, E., Eds.; Wiley-VCH: Weinheim, 2008. (e) *Catalytic Asymmetric Synthesis*, 3rd ed.; Ojima, I., Ed.; Wiley: Hoboken, NJ, 2010.

(4) (a) Martin, R. H. *Chimia* **1975**, *29*, 137. (b) Yokoyama, Y.; Shiozawa, T.; Tani, Y.; Ubukata, T. *Angew. Chem., Int. Ed.* **2009**, *48*, 4521.

(5) (a) Inoue, T.; Matsuyama, K.; Inoue, Y. *J. Am. Chem. Soc.* **1999**, *121*, 9877. (b) Matsuyama, K.; Inoue, T.; Inoue, Y. *Synthesis* **2001**, *8*, 1167.

(6) (a) Green, B. S.; Rabinsohn, Y.; Rejtö, M. *J. Chem. Soc., Chem. Commun.* **1975**, 313. (b) Tolbert, L. M.; Ali, M. B. *J. Am. Chem. Soc.* **1982**, *104*, 1742. (c) Haag, D.; Scharf, H.-D. *J. Org. Chem.* **1996**, *61*, 6127. (d) Saito, H.; Mori, T.; Wada, T.; Inoue, Y. *J. Am. Chem. Soc.* **2004**, *126*, 1900. (e) Saito, H.; Mori, T.; Wada, T.; Inoue, Y. *Chem. Commun.* **2004**, 1652. (f) Saito, H.; Mori, T.; Wada, T.; Inoue, Y. *Org. Lett.* **2006**, *8*, 1909.

(7) (a) Lange, G. L.; Decicco, C.; Tan, S. L.; Chamberlain, G. *Tetrahedron Lett.* **1985**, *26*, 4707. (b) Greene, A. E.; Charbonnier, F. *Tetrahedron Lett.* **1985**, *26*, 5525. (c) Herzog, H.; Koch, H.; Scharf, H.-D.; Runsink, J. *Tetrahedron* **1986**, *42*, 3547. (d) Demuth, M.; Palomer, A.; Sluma, H.-D.; Dey, A. K.; Krüger, C.; Tsay, Y.-H. *Angew. Chem., Int.*

DOI: 10.1021/jacs.5b09775
J. Am. Chem. Soc. 2015, 137, 15007−15014

Ed. Engl. **1986**, *25*, 1117. (e) Lange, G. L.; Decicco, C.; Lee, M. *Tetrahedron Lett.* **1987**, *28*, 2833. (f) Sato, M.; Takayama, K.; Furuya, T.; Inukai, N.; Kaneko, C. *Chem. Pharm. Bull.* **1987**, *35*, 3971. (g) Tsutsumi, K.; Yanagisawa, Y.; Furutani, A.; Morimoto, T.; Kakiuchi, K.; Wada, T.; Mori, T.; Inoue, Y. *Chem. - Eur. J.* **2010**, *16*, 7448.

(8) (a) Gotthardt, H.; Lenz, W. *Angew. Chem., Int. Ed. Engl.* **1979**, *18*, 868. (b) Jarosz, S.; Zamojski, A. *Tetrahedron* **1982**, *38*, 1447. (c) Koch, H.; Runsink, J.; Scharf, H.-D. *Tetrahedron Lett.* **1983**, *24*, 3217. (d) Nehrings, A.; Scharf, H.-D.; Runsink, J. *Angew. Chem., Int. Ed. Engl.* **1985**, *24*, 877. (e) Runsink, J.; Koch, H.; Nehrings, A.; Scharf, H.-D. *J. Chem. Soc., Perkin Trans. 2* **1988**, 49. (f) Buschmann, H.; Scharf, H.-D.; Hoffmann, N.; Plath, M. W.; Runsink, J. *J. Am. Chem. Soc.* **1989**, *111*, 5367. (g) Hegedus, L. S.; Bates, R. W.; Söderberg, B. C. *J. Am. Chem. Soc.* **1991**, *113*, 923. (h) Buschemann, H.; Hoffmann, N.; Scharf, H.-D. *Tetrahedron: Asymmetry* **1991**, *2*, 1429. (i) Matsumura, K.; Mori, T.; Inoue, Y. *J. Am. Chem. Soc.* **2009**, *131*, 17076. (j) Matsumura, K.; Mori, T.; Inoue, Y. *J. Org. Chem.* **2010**, *75*, 5461.

(9) Yang, C.; Ke, C.; Liang, W.; Fukuhara, G.; Mori, T.; Liu, Y.; Inoue, Y. *J. Am. Chem. Soc.* **2011**, *133*, 13786.

(10) Brimioulle, R.; Bach, T. *Science* **2013**, *342*, 840.

(11) (a) Müller, C.; Bauer, A.; Maturi, M. M.; Cuquerella, M. C.; Miranda, M. A.; Bach, T. *J. Am. Chem. Soc.* **2011**, *133*, 16689. (b) Coote, S. C.; Bach, T. *J. Am. Chem. Soc.* **2013**, *135*, 14948. (c) Vallavoju, N.; Selvakumar, S.; Jockusch, S.; Sibi, M. P.; Sivaguru, J. *Angew. Chem., Int. Ed.* **2014**, *53*, 5604.

(12) Nishijima, M.; Goto, M.; Fujikawa, M.; Yang, C.; Mori, T.; Wada, T.; Inoue, Y. *Chem. Commun.* **2014**, *50*, 14082.

(13) (a) Fukuhara, G.; Nakamura, T.; Yang, C.; Mori, T.; Inoue, Y. *J. Org. Chem.* **2010**, *75*, 4307. (b) Fukuhara, G.; Nakamura, T.; Yang, C.; Mori, T.; Inoue, Y. *Org. Lett.* **2010**, *12*, 3510. (c) Fukuhara, G.; Nakamura, T.; Kawanami, Y.; Yang, C.; Mori, T.; Hiramatsu, H.; Dan-oh, Y.; Tsujimoto, K.; Inoue, Y. *Chem. Commun.* **2012**, *48*, 9156. (d) Fukuhara, G.; Nakamura, T.; Kawanami, Y.; Yang, C.; Mori, T.; Hiramatsu, H.; Dan-oh, Y.; Nishimoto, T.; Tsujimoto, K.; Inoue, Y. *J. Org. Chem.* **2013**, *78*, 10996.

(14) Bradbrook, G. M.; Gessler, K.; Côté, G. L.; Momany, F.; Biely, P.; Bordet, P.; Pérez, S.; Imberty, A. *Carbohydr. Res.* **2000**, *329*, 655.

(15) Demchenko, A. V.; Pornsuriyasak, P.; Meo, C. D. *J. Chem. Educ.* **2006**, *83*, 782.

(16) Suzuki, S.; Fujii, T.; Yamanaka, S.; Yoshiike, N.; Hayashi, Z. *Bull. Chem. Soc. Jpn.* **1979**, *52*, 742.

(17) (a) Harada, N.; Nakanishi, K. In *Circular Dichroic Spectroscopy—Exciton Coupling in Organic Stereochemistry*; University Science Books: Mill Valley, CA, 1983. (b) Berova, N.; Bari, L. D.; Pescitelli, G. *Chem. Soc. Rev.* **2007**, *36*, 914.

(18) De Schryver, F. C.; Collart, P.; Vandendriessche, J.; Goedeweeck, R.; Swinnen, A.; Van der Auweraer, M. *Acc. Chem. Res.* **1987**, *20*, 159.

(19) Nehira, T.; Parish, C. A.; Jockusch, S.; Turro, N. J.; Nakanishi, K.; Berova, N. *J. Am. Chem. Soc.* **1999**, *121*, 8681.

(20) De Schryver, F. C.; De Brackeleire, M.; Toppet, S.; Van Schoor, M. *Tetrahedron Lett.* **1973**, *15*, 1253.

(21) (a) Chandross, E. A.; Ferguson, J. *J. Chem. Phys.* **1966**, *45*, 3564. (b) Fielding, P. E.; Jarnagin, R. C. *J. Chem. Phys.* **1967**, *47*, 247. (c) Mataga, N.; Torihashi, Y.; Ota, Y. *Chem. Phys. Lett.* **1967**, *1*, 385. (d) Kaanumalle, L. S.; Gibb, C. L. D.; Gibb, B. C.; Ramamurthy, V. *J. Am. Chem. Soc.* **2005**, *127*, 3674.

(22) Nakamura, A.; Inoue, Y. *J. Am. Chem. Soc.* **2003**, *125*, 966.

(23) Dimroth, K.; Reichardt, C.; Siepmann, T.; Bohlmann, F. *Liebigs Ann. Chem.* **1963**, *661*, 1.

(24) Wakai, A.; Fukasawa, H.; Yang, C.; Mori, T.; Inoue, Y. *J. Am. Chem. Soc.* **2012**, *134*, 4990 and 10306 (erratum).

(25) Grimme, S. *J. Phys. Chem. A* **2005**, *109*, 3067.

DOI: 10.1021/jacs.5b09775
J. Am. Chem. Soc. 2015, 137, 15007−15014